
# *Comparison of the sedimentologic and stratigraphic characteristics of the Point Lookout vs. Gallup sandstones near Cabezon, New Mexico*

Daniel J. Koning, [ed.]
2024, pp. 201-217. https://doi.org/10.56577/FFC-74.201
Supplemental data: https://nmgs.nmt.edu/repository/index.cfml?rid=2024005

*in:*

*Geology of the Nacimiento Mountains and Rio Puerco Valley*, Karlstrom, Karl E.;Koning, Daniel J.;Lucas, Spencer G.;Iverson, Nels A.;Crumpler, Larry S.;Aubele, Jayne C.;Blake, Johanna M.;Goff, Fraser;Kelley, Shari A., New Mexico Geological Society 74 th Annual Fall Field Conference Guidebook, 334 p.

*This page is intentionally left blank to maintain order of facing pages.*

New Mexico Geological Society Guidebook, 74th Fall Field Conference, 2024, p. 201–217, https://doi.org/10.56577/FFC-74.201


# COMPARISON OF THE SEDIMENTOLOGIC AND STRATIGRAPHIC CHARACTERISTICS OF THE POINT LOOKOUT VS. GALLUP SANDSTONES NEAR CABEZON, NEW MEXICO

DANIEL J. KONING

New Mexico Bureau of Geology and Mineral Resources, 801 Leroy Place, Socorro, NM 87801; dan.koning@nmt.edu

**Abstract**—Using three stratigraphic sections, this paper compares the sedimentologic and stratigraphic characteristics of the Point Lookout (early Campanian, 84–81 Ma) and Gallup (early Coniacian, 90–89.5 Ma) sandstone tongues near Cabezon, New Mexico. Each of these tongues represents a major regression event along the southwestern shoreline of the Western Interior Seaway, exhibiting progressive upward coarsening and shallowing trends. Two differences are noted. First, lenticular and channel-shaped, >20-cm-thick sandstone beds with basal scour features (e.g., toolmarks, gutter casts) are common in the lower Point Lookout Sandstone and its lower transition with the Mancos Shale, but they are very sparse in the Gallup Sandstone. In the Point Lookout Sandstone, the orientation of channel fills and toolmarks in these and overlying, tabular beds range from 340° to 020° (mostly north-northeast), which is orthogonal (and to a lesser extent, left-oblique) to the northwestern-trending coastline and likely reflects periodic storm-related, offshore-directed currents. Second, 5th-order parasequences are more obvious in the Point Lookout Sandstone, where laterally continuous mudstones (up to 3 m thick) transition upwards into sandstones, resulting in mudstone-sandstone couplets that indicate deepening (transgression) followed by shallowing (regression). These mudstone-sandstone couplets are absent in the Gallup Sandstone, and except for the transitional base and lower part of this unit, individual parasequences are more obscure. There is also a lack of upward coarsening in the middle to upper part of the Gallup Sandstone. Differences in shoreline morphology controlled by contrasting sea-level stages that relate to systems tracts, as modeled by sequence stratigraphy, may explain the observed differences. The Point Lookout Sandstone has an aggradation-progradation accommodation (stacking) succession and previously was interpreted as deposited in a highstand systems tract. During transgressions, sand was captured by lagoons and estuaries that resulted in sand-starved, muddy deposition on the shoreface ramp. Organic detritus in marine shales and along sandstone bedding planes is consistent with nearby delta distributary channels, which likely facilitated storm-flood currents and related deposition. In contrast, the middle-upper Gallup at Guadalupe Ruin has a progradation-aggradation stacking succession; its middle-upper part is inferred to have aggraded in a late stage of a lowstand system tract with slowly rising sea level. A corresponding coastline with incised river valleys on the coastal plain, increased shore-parallel transport of sand, and a lack of lagoons and estuaries resulted in a high volume of sand input to the nearshore environment. The high sand flux may have inhibited development of thick, transgressive mudstones during high-frequency (5th-order) transgressive events. Relatively long distances to deltaic distributary channels, not necessarily related to low sea levels but perhaps happenstance, may explain the paucity of paleochannel, gutter casts, and toolmark features in the Gallup Sandstone at Guadalupe Ruin.

## INTRODUCTION

### Late Cretaceous Stratigraphy and Paleogeographic Setting

The Western Interior Seaway (WIS) covered the interior of North America during the Late Cretaceous, effectively connecting the Gulf of Mexico with the Arctic Ocean. Part of the western shoreline of the WIS extended across New Mexico, where it trended northwest-southeast and was characterized by barrier islands, strand plains (broad shorelines with well-defined parallel sand ridges separated by shallow swales), deltas related to small- to medium-sized drainages ($10^2$ to $10^5$ km$^2$ per Van Cappelle et al., 2018, and Lin and Bhattacharya, 2020), tidal flats, and lagoons (Fig. 1; Shetiwy, 1978; Wright, 1986; Devine, 1991; Wright-Dunbar, 1992; Wright-Dunbar et al., 1992; Katzman and Wright-Dunbar, 1992; Nummedal, 2004; Zeck, 1982). In New Mexico, the WIS reached its maximum extent during the late Cenomanian through earliest Turonian (96–93 Ma) and progressively shrank until it left the state at ~70 Ma. Superimposed on this long-term, eastward retreat ($10^7$ yr) were shorter term sea-level oscillations resulting in 3rd-order transgressive-regressive events. These events produced progradational sandstones exhibiting nearshore facies that intertongue with marine mudstones assigned to the Mancos Shale.

This study compares two of these nearshore sandstone tongues, the Point Lookout and Gallup Sandstones, in the middle Rio Puerco Valley near the ghost town of Cabezon, located 3 km to the northeast of Cabezon Peak in northwestern New Mexico (Figs. 1–3). This area lies in the southeastern part of the Colorado Plateau, 70 km northwest of Albuquerque (Fig. 1). There, as elsewhere on the Plateau, intervening nearshore sandstone tongues are each formally named and characteristically terminate to the northeast (seaward) in the marine Mancos Shale and grade landward (southwest) into terrestrial deposits (Fig. 3). In the area around Cabezon, the exposed stratigraphic units of the WIS include, in ascending order and with approximate thicknesses: lower tongue of Mancos Shale, Gallup Sandstone (18 m); Mulatto Tongue of Mancos Shale (155 m), Dalton-Hosta sandstone tongue (12–15 m), Satan Tongue of Mancos Shale (95 m), and Point Lookout Sandstone (22 m). (The thickness of the Mulatto Tongue is from comparing Google Earth elevations parallel to stratal strike, and other

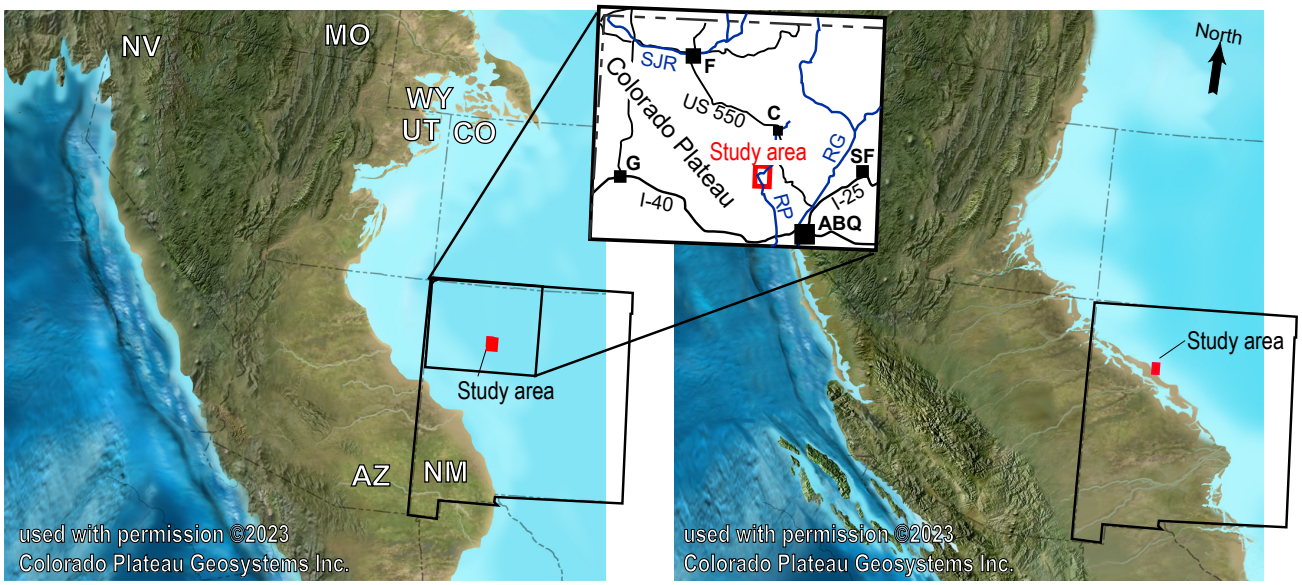


FIGURE 1. Paleogeography of the southwestern United States at about the time of deposition of the Gallup Sandstone (left panel) and Point Lookout Sandstone (right panel). The study area is shown by a red rectangle relative to state boundaries. The inset at top-center shows the study area (red rectangle) relative to cities, highways, and rivers in northwestern New Mexico. State abbreviations: AZ = Arizona, CO = Colorado, MO = Montana, NM = New Mexico, NV = Nevada, UT = Utah. City abbreviations (black text): ABQ = Albuquerque, C = Cuba, F = Farmington, G = Gallup, SF = Santa Fe. River abbreviations (blue text): RG = Rio Grande, SJR = San Juan River, RP = Rio Puerco. Paleogeographic maps are used with an academic content license agreement from Colorado Plateau Geosystems Inc.

thicknesses are from this study and unpublished data from D.J. Koning). The Point Lookout Sandstone has back-barrier facies near its top (e.g., lagoon, estuary, and tidal channel facies) that grade upward into coal-bearing, terrestrial deposits of the Menefee Formation (Wright and Hayden, 1988; Devine, 1991; Katzman and Wright-Dunbar, 1992). The youngest and final marine tongue in the Late Cretaceous succession, the Lewis Shale (not shown in Fig. 3), outcrops ~20 km north of the town of San Luis. Biostratigraphic data (i.e., ammonites and inoceramids) indicate that the Gallup Sandstone near Cabezon is earliest Coniacian (*Scaphites preventricos* ammonite zone) and the Point Lookout Sandstone is early Campanian (above or in the *Scaphites hippocrepis* ammonite zone; Sealey and Lucas, 2019; P. Sealey, written comm., 2024). Figure 4 compares the age control for the Point Lookout and Gallup Sandstones with global stratigraphic sequences and eustatic curves.

## Sequence Stratigraphy

Elements of sequence stratigraphy relevant to this paper include parasequences and sequence tracts (van Wagoner et al., 1987, 1988; Posamentier et al., 1988; SEPM, 2024). Stereotypical parasequences in siliciclastic sediment are repeated, upward-coarsening units bound by discrete flooding surfaces. A systems tract comprises a related system of depositional facies that may include back-barrier environments (tidal flats and lagoons), barrier islands, nearshore environments (foreshore, upper shoreface, proximal lower shoreface, and distal lower shoreface), and relatively deep-water, offshore environments. The three main systems tracts used in this paper include highstand, lowstand, and transgressive sequence tracts (HST, LST, and TST); these systems tracts, important related stratigraphic surfaces, and their relationships with sea-level changes are summarized in Figure 5 and reviewed in SEPM (2024).

## Stratigraphic Context of Gallup and Point Lookout Sandstones

### Gallup Sandstone

Although several tongues of the Gallup Sandstone are noted near Gallup, its type area (Sears, 1925), only one tongue is seen in the middle Rio Puerco Valley. This ~18-m-thick tongue (as measured in this study) is correlative to the A tongue depicted in Nummedal and Molenaar (1995). The finding of *Scaphities preventicos* at the top of the Gallup Sandstone in the Cabezon area (Sealey and Lucas, 2019) indicates an early Coniacian age of 89.5–90.0 Ma, consistent with youngest Gallup deposition (Nummedal and Molenaar, 1995). The age of the A tongue corresponds to a globally recognized, sea-level lowering (~70 m) and corresponding progradation of nearshore sandstones (Fig. 4).

The Gallup Sandstone represents the first major progradation in the Upper Cretaceous section of the San Juan Basin (Molenaar, 1983) and is inferred to be near a deltaic complex (Gardner, 1995; Nummedal and Molenaar, 1995; Lin and Bhattacharya, 2021). The Gallup Sandstone crops out near the Rio Puerco about 8 km south of Cabezon Peak (near the ghost town of Guadalupe; Fig. 2) and on the eastern side of Mesa Prieta (southeast of Fig. 2 map area), pinching out to the northeast before the main drainage of the Rio Salado. The Gallup Sandstone tongue overlies the lower tongue of the Mancos

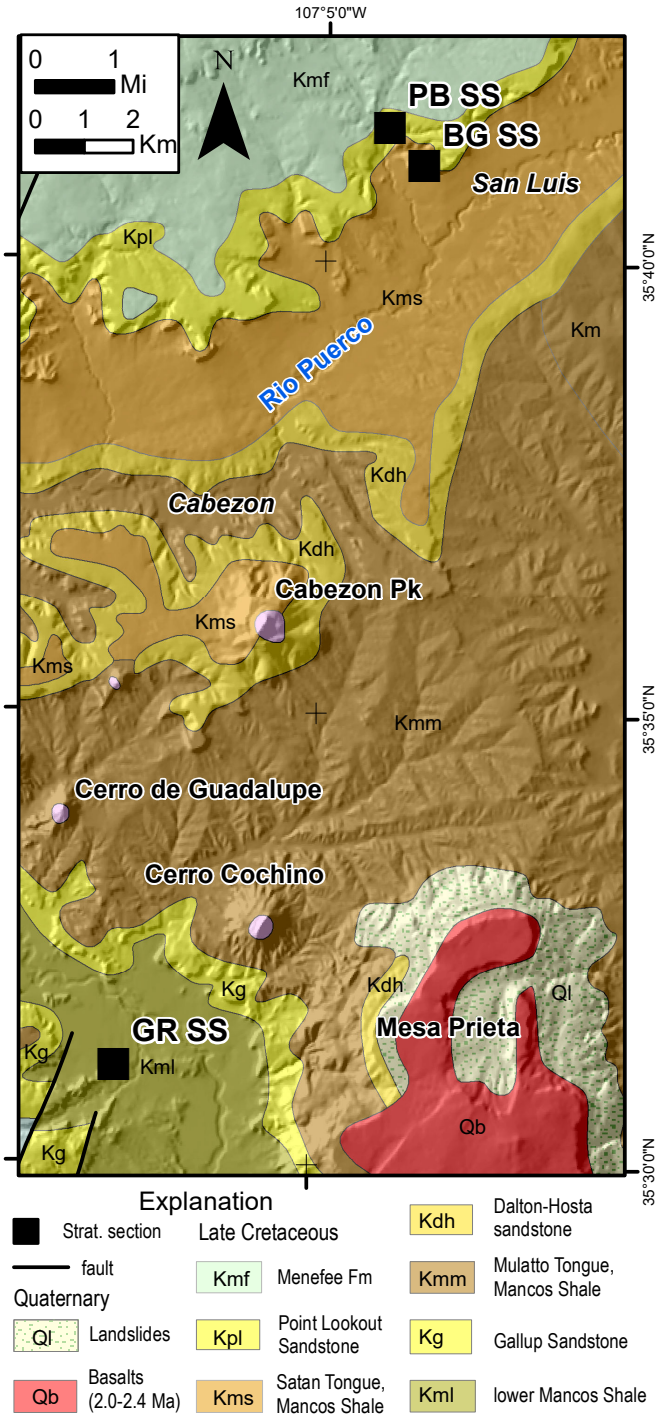


FIGURE 2. Geologic map of the Cabezon area. New stratigraphic sections described in this paper for the Point Lookout and Gallup Sandstones, respectively, are labeled Bosque Grande (BG SS) and Guadalupe Ruin (GR SS) and shown as black squares. A previous stratigraphic section of the Point Lookout Sandstone—the Point Balcon section (PB SS) from Wright and Hayden (1988)—is also shown. The geology is slightly modified from New Mexico Bureau of Geology and Mineral Resources (2003). Fm = formation.

Shale. The Gallup is locally overlain in a seaward direction by the marine Tocito Sandstone. The upper Gallup Sandstone grades landward into the nonmarine Dilco Coal Member of the Crevasse Canyon Formation (Fig. 3). The Gallup coastal margin has been interpreted as a low-gradient, basinal ramp margin setting with shallow water (<200 m water depth; Nummedal, 1990). Previous works on lithofacies and depositional environments of the Gallup include Molenaar (1973, 1983), Campbell (1971, 1973, 1979), Tillman (1985), Nummedal and Swift (1987), and Nummedal (1990). Studies addressing sequence stratigraphic topics include Weimer (1984), Nummedal (1990), Nummedal and Riley (1991), Nummedal and Molenaar (1995), and Nummedal (2004). Particularly important to this paper are the detailed stratigraphic investigations by Lin et al. (2019) and Lin and Bhattacharya (2020, 2021), who measured and described 71 closely spaced stratigraphic sections across an outcrop belt ~200 km west of Cabezon. For the Gallup Sandstone and interbedded marine mudstones, Lin et al. (2019) identified 16 depositional facies associations and subdivided the studied strata into 61 individual parasequences, comprising 26 parasequence sets and 12 sequences.

## Point Lookout Sandstone

The Point Lookout Sandstone represents a major northeastward progradation of the shoreline in the early Campanian. Its nearshore sandstones are capped by back-barrier facies (e.g., lagoon, estuary, tidal channels) and are overlain by (and correlate landward southwestward with) coastal swamp and plain deposits of the Cleary Coal Member of the Menefee Formation (Wright, 1986; Devine, 1991; Wright-Dunbar, 1992; Nummedal and Molenaar, 1995, fig. 1). A fossil of *Scaphites hyppocritus I* has been found in the uppermost Satan Tongue below the Point Lookout, indicating that progradation of the Point Lookout occurred no earlier than 84 Ma, probably in the *Scaphites hyppocritus II and III* ammonite zones that are 84–81 Ma (Fig. 4; Sealey and Lucas, 2019). Interestingly, there is no notable drop in global sea levels at this time (Haq, 2014; Fig. 4). Sedimentologic-stratigraphic work on the Point Lookout Sandstone was pioneered in the Cabezon area by Wright (1986), who noted high-frequency transgression-regression intervals (5th-order parasequences) in nearshore environments. Her later studies noted that the top of a parasequence commonly fines upward, rather than having a sharp lithologic contact (Wright and Hayden, 1988; Wright-Dunbar, 1992). Investigations of a slightly more landward position of the Point Lookout (Devine, 1990; Katzman and Wright-Dunbar, 1992) discovered that tidal flats and lagoon facies correlate laterally to transgressive events in the nearshore record, which was explained by rising sea levels drowning river valleys and tidal flats with minimal landward retreat (Devine, 1991; Katzman and Wright-Dunbar, 1992). Regressive downlap in the ensuing sea-level drop resulted in a relatively abrupt coarsening of strata above these transgressive deposits (Wright-Dunbar, 1992).

## Purpose

In reconnaissance geologic investigations, I noted sedimentologic differences between the three aforementioned sandstone tongues in the Cabezon area, prompting this more detailed study. Using three stratigraphic sections (Fig. 2), this paper documents and compares the lithologic character of

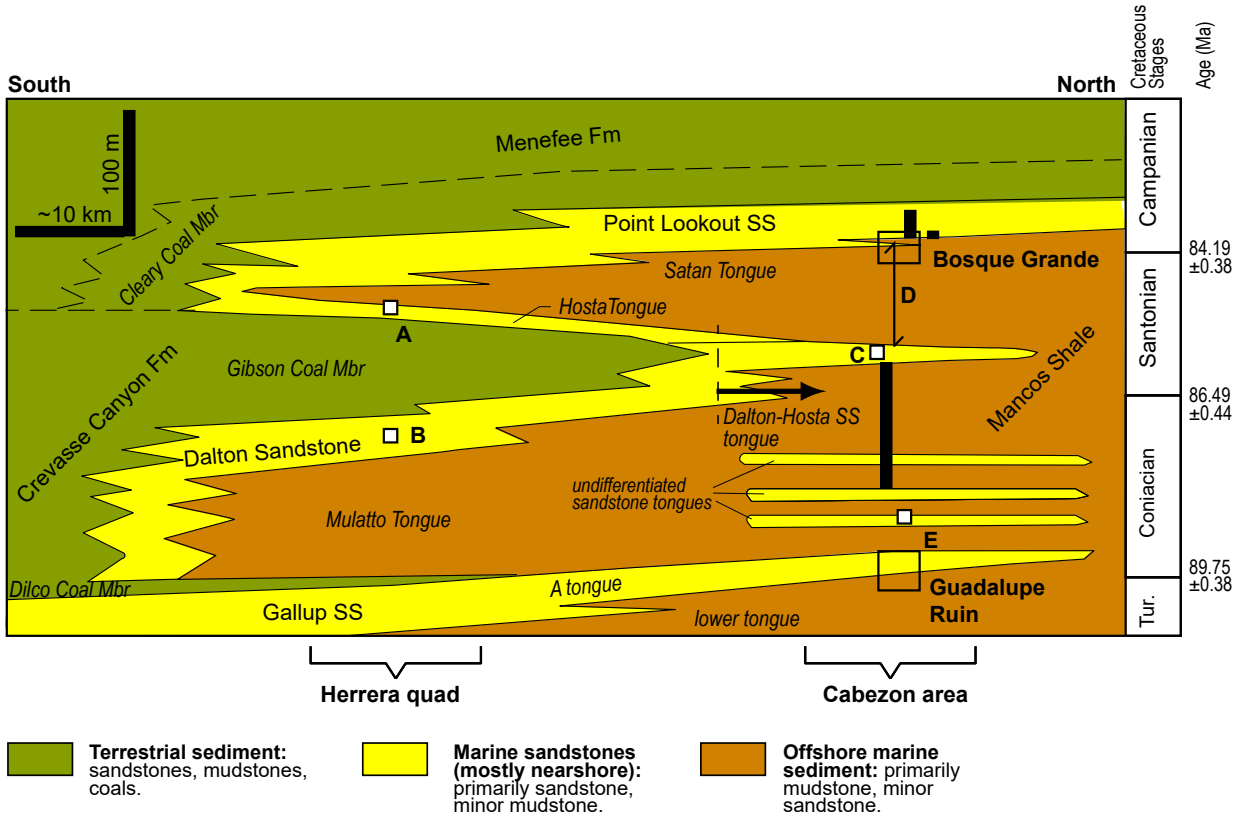


FIGURE 3. Schematic north-south cross section illustrating the Late Cretaceous stratigraphy of the Rio Puerco Valley between Interstate 40 and San Luis. Note that the trend of the section is oblique to the northwest-southeast trending paleoshoreline. Thicknesses and stratigraphic relations from the Herrera quadrangle (~16 km north of Interstate 40) are from the geologic mapping of Rawling and Koning (2019), Koning and Rawling (2017), and Koning and Jochems (2014). General thicknesses and stratigraphic relations in the Cabezon area are from Hunt (1936), New Mexico Bureau of Geology and Mineral Resources (2003), this study, and D.J. Koning (unpublished data). Thickness of the Mulatto Tongue is from measurements in Google Earth and has an estimated 10 m error. Ages for Late Cretaceous stages are from Singer et al. (2023). Age and thicknesses at specific localities (white boxes labeled A through E) are from: (A) Bourdon et al. (2011), (B) Johnson and Lucas (2003), (C and D) Koning (unpublished data), and (E) Williamson and Lucas (1992).

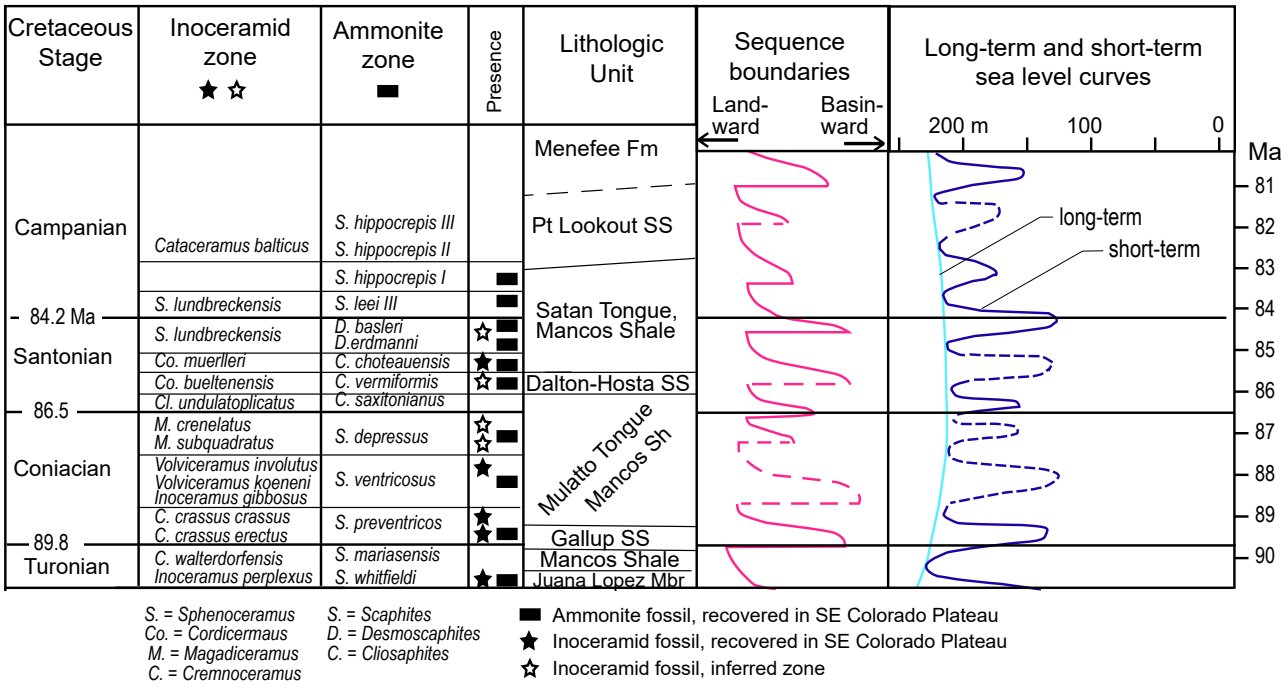


FIGURE 4. Comparison of age control, North American sequences, and long-term and short-term sea-level curves for Upper Cretaceous strata exposed near Cabezon. Ammonite and inoceramid data are from Sealey and Lucas (2019). Sequence boundaries and sea-level curves are from Haq (2014). Cretaceous stage ages are modified from Sealey and Lucas (2019) according to Singer et al. (2023).

two of these sandstone tongues, the Gallup and Point Lookout Sandstone. For more information and discussion of the Dalton-Hosta Sandstone, refer to Optional Stop 2 of the Second-Day Road Log (Koning et al., 2024). I present a working hypothesis that appeals to sea-level-controlled differences in shoreline morphometry and proximity to deltaic distributary channels to explain these sedimentologic differences.

## OBSERVATIONS AND FACIES INTERPRETATIONS

Two stratigraphic sections were measured and described in locations coinciding with Stops 1 and 3 on the 2024 NMGS Fall Field Conference Second-Day Road Log (Fig. 2). The two stratigraphic sections were measured using an Abney level and hand-held GPS: Bosque Grande in the Point Lookout Sandstone (abbreviated as BG SS in Fig. 2) and Guadalupe Ruin in the Gallup Sandstone (abbreviated as GR SS in Fig. 2). Described features include bedding thickness and geometry, contacts, and grain size. Ichnofossils were noted, and orientations of toolmarks were measured. Aside from local bivalve molds, no invertebrate fossils were found. Descriptive data for the stratigraphic sections are presented in Appendix 1. This study also refers to a previous stratigraphic section measured 0.4 km north of Stop 1B of the Second-Day Road Log (Wright and Hayden, 1988, abbreviated as PB SS on Fig. 2). Photographs presented below document stratigraphic architecture and lithologic character. Depositional environments are assigned according to the criteria listed in Table 1.

### Gallup Sandstone (Guadalupe Ruin Stratigraphic Section)

### Lithology

The Gallup Sandstone at Guadalupe Ruin is characterized

TABLE 1. Criteria for interpretation of depositional environments

| Environment | Lithology | Sedimentary structures | Other* |
|---|---|---|---|
| Tidal channel & related delta | Lower-fine to lower-coarse-grained, cross-bedded sandstones | Ripple cross-lamination, tabular bedding, herringbone cross-lamination. | *Skolithos*. Low to intense bioturbation. Fining upward intervals. Abundant wood and coal chips. |
| Lagoon | Mudstone-dominated, with variable lower-very-fine to lower-fine-grained sandstones | Thinly bedded, or massive due to bioturbation. Common ripple cross-lamination and horizontal-planar laminations. | Low to intense bioturbation |
| Barrier island | Lower-fine to upper-medium-grained sandstone | >0.5-m-thick dune cross-stratification; local tabular sandstone and bioturbated sandstones | *Skolithos*. Absent to intense bioturbation. |
| Distributory channel | Upper-fine to lower-coarse-grained sandstones | Trough to planar cross-bedded; locally tabular sandstones. Bar forms with limited extent. | *Skolithos*. Absent to sparse bioturbation. Paleocurrent orthogonal to shorelines. Mudstone drapes on SS. Abundant mud rip-ups, wood chunks, and coaly chips. |
| Foreshore | Fine- to medium-grained sandstone. Heavy mineral concentrations. | Planar to sub-planar beds dipping seaward | Absent to sparse biotrbation |
| Upper shoreface | Lower-fine- to lower-coarse-grained sandstone, mostly fine-upper to medium-grained. | Cross-bedded (trough and planar foresets) and tabular-bedded. Bed thicknesses 0.5–3 m. Longshore trough deposits. | *Skolithos*. Absent to sparse bioturbation. Multidirectional paleoflow. Contact with lower shoreface is marked by abrupt grain-size change or scour. |
| Proximal lower shoreface | Lower-very-fine to lower-fine-grained sandstones. Lacks mudstone beds, and sandstone beds tend to be amalgamated. | HCS, SCS, and planar to low-angle cross-bedding; ripple cross-lamination. Laminated SS interbedded with bioturbated sandstone beds; bed thickness up to 1 m. | *Skolithos*. Absent to thorough bioturbation. Abundant gutter casts at base of beds. |
| Distal lower shoreface | Muddy to silty, lower- to upper-very-fine-grained sandstones, thin tempestite sandstones | Intensely bioturbated and difficult-to-see red structures; only remnant ripple- to low-angle cross lamination, HCS, and SCS. | Moderate to thorough bioturbation. Plant and organic matter common. |
| Offshore transition | Silty to sandy mudstones and sandy siltstones; subordinate vf SS (often tempesites) | Centimeter-scale, thin bedded, planar bedding. Local HCS. Tempesites internally masive & have scoured bases. Bouma sequences common. | Absent to thorough bioturbation. As a whole, coarsens upward. Abundant organic matter and shell fragments. |
| Offshore | Dark (organic-rich), clayey mudstones and shales; subordinate silty mudstones-muddy siltstones | Centimeter-scale bedding that is internally massive, laminated, or normally graded. | Absent to thorough bioturbation. Abundant organic matter and shells. |

**Notes:**
Criteria summarized from Lin et al. (2019) and Pemberton et al. (2012).
SS = sandstone; HCS = hummocky cross-stratification; SCS = swaly cross-stratification
* Ichnofossil criteria were not heavily employed in this study.

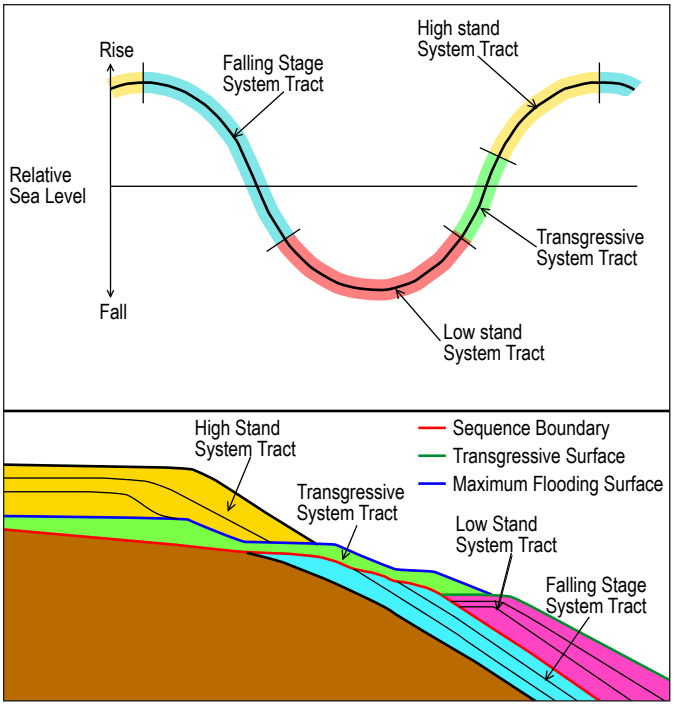


FIGURE 5. Schematic diagram illustrating systems tracts and surfaces related to sequence stratigraphy. From Wright (2013) and OpenGeology.org (https://opengeology.org/historicalgeology/tools-of-historical-geology/stratigraphic-tools-basic-sequence-stratigraphy/).

by a cliff-forming, 18-m-thick interval of amalgamated sandstone. This sandstone conformably overlies the Mancos Shale across a 4-m-thick transition zone. Noteworthy stratigraphic intervals are described below in ascending order. Annotated photographs of the measured outcrop are shown in Figures 6 and 7, and the stratigraphic section is presented in Figure 8.

The Mancos Shale is assigned to the lower 9.9 m of the Guadalupe Ruin section and consists of interbedded mudstones, siltstone, and minor very fine sandstone (Figs. 6 and 8). Strata are tabular and laminated to very thinly bedded. This interval contains 10–20% ledge-forming beds (up to 10 cm thick) composed of lower-very-fine to lower-fine sandstone. Sandstone beds have sharp bases and tops and commonly have clayey interlamina. The minor presence of sandstones and silty nature of the mudstones suggest a transitional offshore-lower shoreface environment. A distinctly hummocky cross-stratified sandstone bed in the lower 0.4 m of the stratigraphic section may denote the top of an underlying parasequence or a storm-related depositional event (Fig. 8; Lin and Bhattacharya, 2021). Parasequence (P-1) is about 8 m thick, extending across the measured Mancos Shale interval, and capped by a 10-cm-thick, relatively continuous bed of upper-very-fine to lower-fine sandstone (Fig. 8, unit 3b).

Between the Gallup Sandstone and Mancos Shale is a 4-m-thick transitional zone (Figs. 6–8, units 3d–3e through 4), characterized by interbedded, very fine- to fine-grained

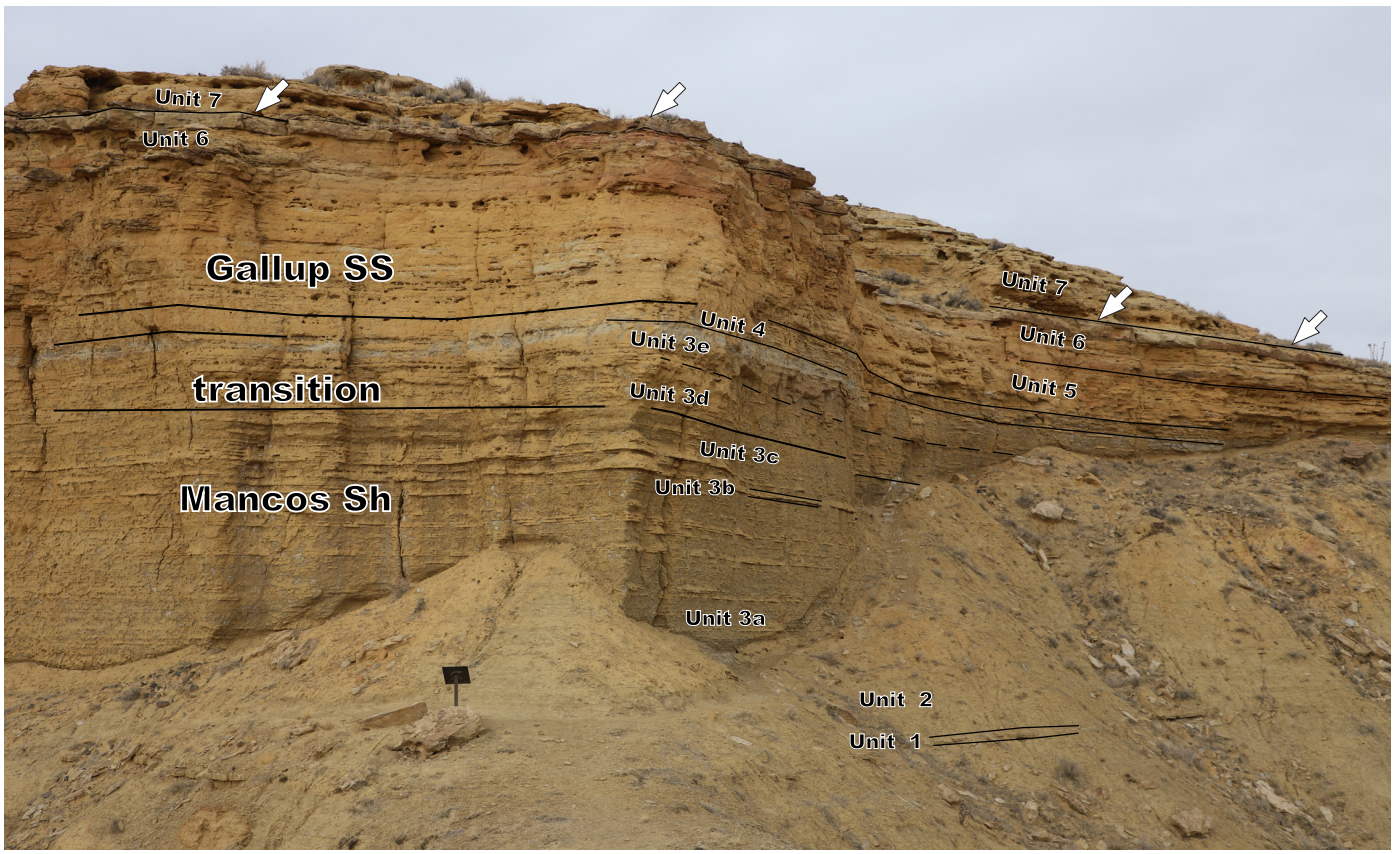


FIGURE 6. Annotated outcrop corresponding to the lower-middle part of the Guadalupe Ruin stratigraphic section. View is to the west. Units correspond to those depicted in the stratigraphic section of Figure 8. The sharp, laterally extensive contact at the top of the sandstone bed capping Unit 6 (white arrows) may possibly correspond to a sequence boundary between parasequences P-2 and P-3 (Fig. 8) that correlates to the sequence boundary shown in Figure 14 between the lowstand and highstand system tracts.

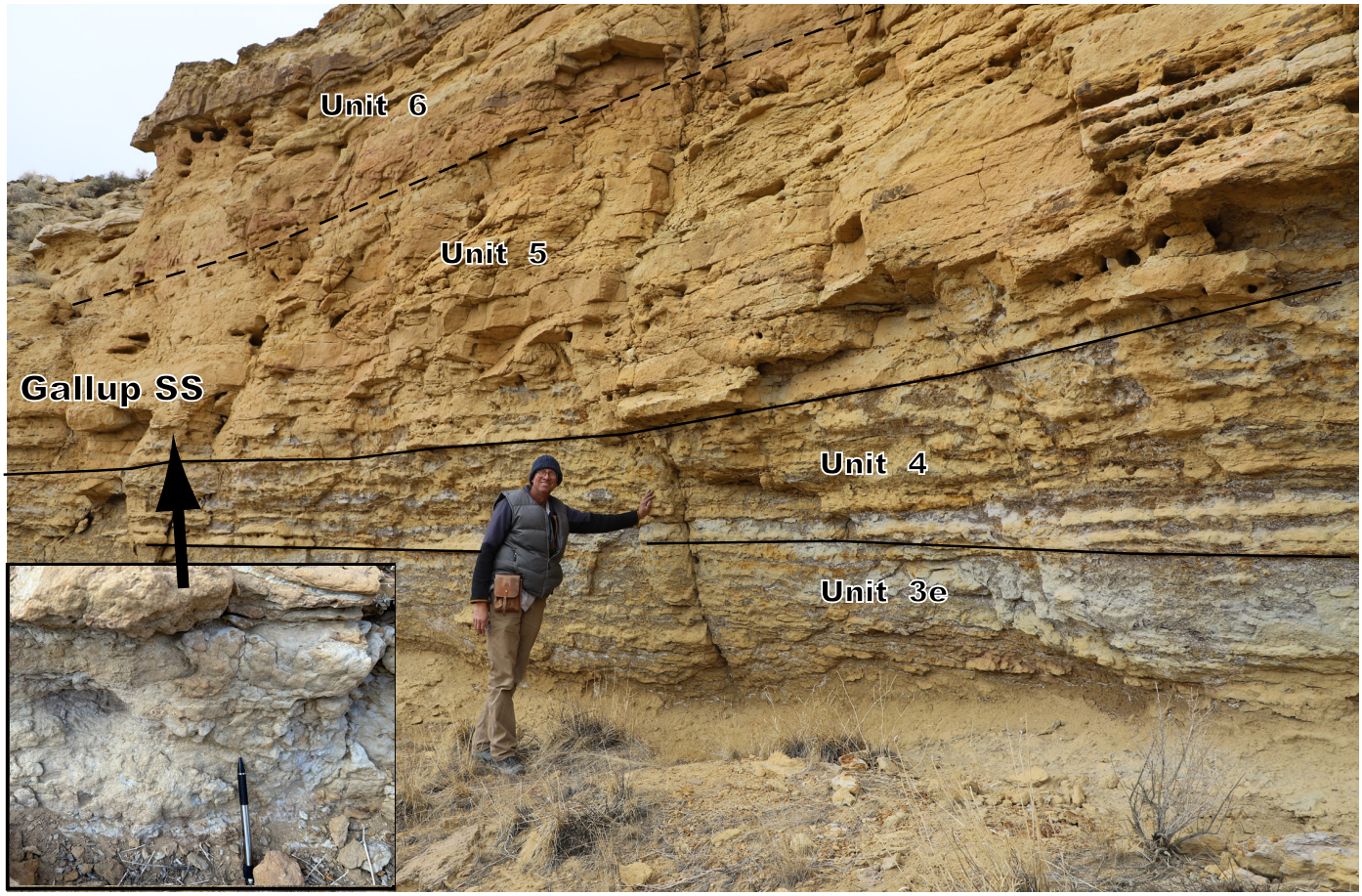


FIGURE 7. Close-up photograph of the transitional base of the Gallup Sandstone. Note the tabular bedding and lack of deep paleochannels. Burrowing occurred in this transitional zone and at the base of the overlying unit 5 (inset photograph). Units correspond to those depicted in the stratigraphic section of Figure 8. The man is 1.95 m tall.

sandstones and subordinate silty mudstones. The proportion of sandstone beds increases upsection, from 20–30% to 80–90%, and general bedding thickness also increases slightly upward. Notable burrowing is evident in units 3e and 4, with burrows appearing to localize diagenetic oxidation and cementation. Based on the dominance of sandstone and the high intensity of bioturbation, I assigned the transitional zone to the distal lower shoreface depositional environment (Table 1).

Above the basal transition zone, the Gallup Sandstone consists of thin to thick, tabular beds of predominantly fine-grained sandstone (Fig. 8, units 5–10). The sand is tan to yellowish tan, subangular to subrounded, well sorted, and composed of quartz with 1–5% dark mafic grains and/or chert. Most beds lack sedimentary structures (are massive), and bulbous (knobby) outcrop surfaces suggest former burrows, which are most obvious in the lower and upper meter (Figs. 7 and 8, base of unit 5 and unit 10). No mudstone interbeds are present.

In the Gallup Sandstone, a few noteworthy intervals are defined by changes in bedding or grain size. The lower 1.3 m (Fig. 8, lower-middle unit 5) has the finest sand (mostly lower-fine grain size) and consists of very thin to thin, heavily bioturbated sandstone (Figs. 7 and 8); the upper 0.6 m of unit 5 gradually coarsens upward into the overlying unit 6. Unit 6 (~2 m thick) exhibits locally distinct, horizontal-planar lamination occurring within thin, tabular beds; grain size is mostly upper-fine (minor lower-medium). Overlying sandstones (units 7, 8, 10) are mostly thickly bedded and massive (bioturbated), and grain sizes range from lower-fine to lower-medium; however, a few meters below the top is a distinctive interval (unit 9), notable for its golden-yellow color, thin bedding, slightly finer sand, and high amount of bioturbation.

The most obvious parasequence in the Guadalupe Ruin stratigraphic section (Parasequence 2, or PG-2) spans the transitional base of the Gallup Sandstone. Parasequence 2 exhibits a 10-m-thick, coarsening-upward trend spanning units 3c through 6 (Fig. 8). In addition to sand coarsening upward (upper-very-fine and lower-fine near the bottom versus upper-fine and lower-medium near the top), bioturbation intensity decreases upsection. I interpret that Parasequence 2 represents an upward progression from mudstone-dominated, transitional offshore strata (unit 3c) to amalgamated sandstones shallower in the proximal lower shoreface (units 5, 6).

The overlying sandstone (Fig. 8, units 7–10) may possibly be divided into two cryptic parasequences called 3a and 3b (Fig. 8), each about 5–8 m thick; note that 3a and 3b may actually constitute a single parasequence. The wholly sandstone nature of the middle-upper Gallup Sandstone (units 7–10), in addition to the high amount of bioturbation and only local horizontal

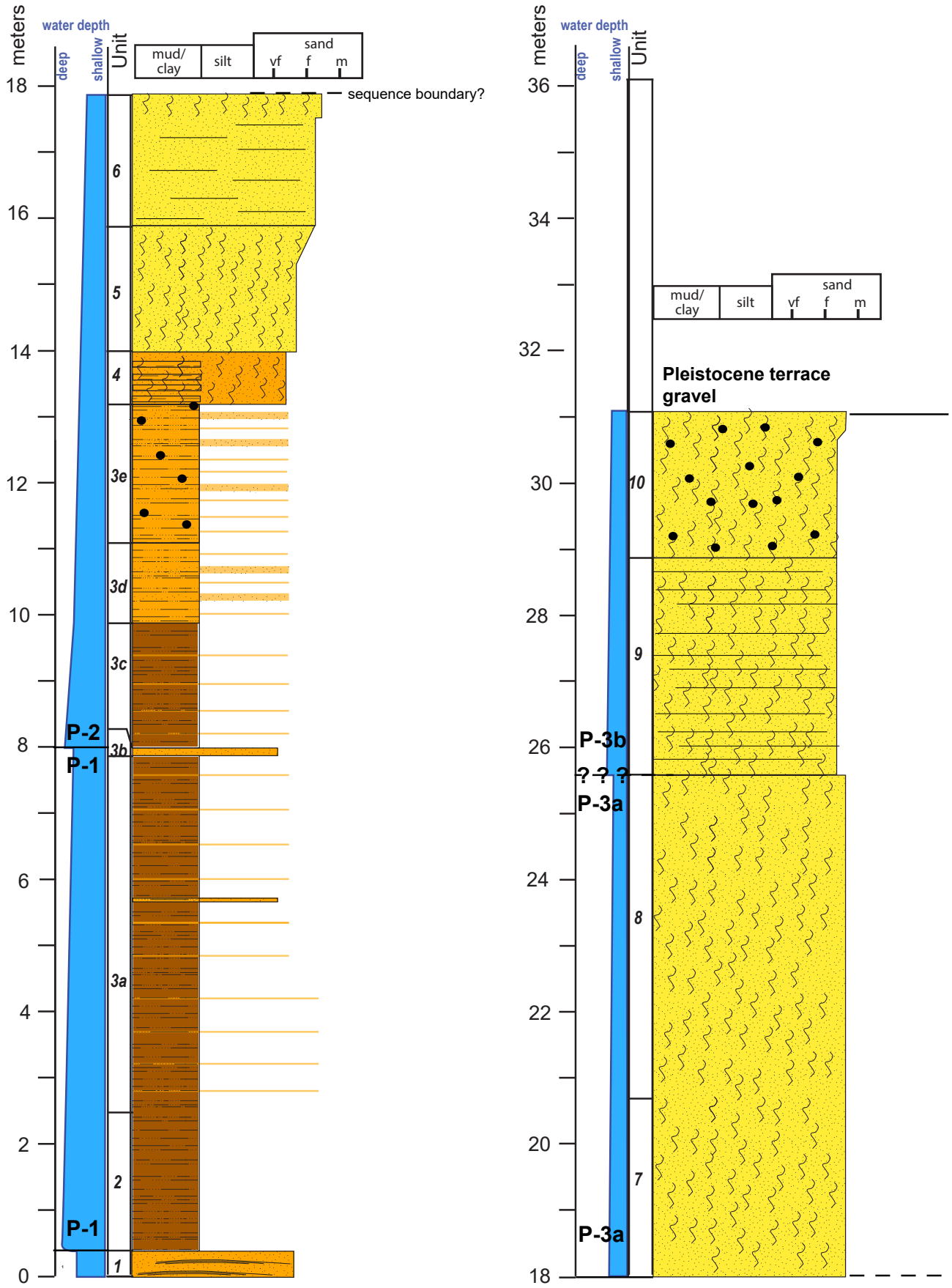


FIGURE 8. Guadalupe Ruin stratigraphic section. Inferred relative water depth is shown on the left side of the graphic column. P-1, P-2, P-3a, and P-3b are interpreted parasequences (P-3a and P-3b may represent a single parasequence). Explanation of symbols is given in Figure 12.

to swaly laminations, suggest a relatively low-energy, lower shoreface environment with only minor upsection water-depth changes. It is probably near the middle of the lower shoreface, lacking both the muddy sandstones expected of the distal lower shoreface and the cross-stratification characterizing the proximal lower shoreface and upper shoreface (Table 1).

### Point Lookout Sandstone (Bosque Grande Stratigraphic Section)

The main body of the Point Lookout is a ~22-m-thick, amalgamated, fine-grained sandstone that overlies a 3–4-m-thick, mudstone-dominated interval informally known as the "marker shale" (T2, Figs. 9 and 10). Another mudstone interval (T3) lies about halfway up the main body. Both mudstones extend several kilometers and have been interpreted to reflect high-frequency ($10^4$–$10^5$ m.y.) transgressions (Wright, 1986; Wright-Dunbar, 1992; Wright and Hayden, 1988). Between the T2 and T3 units and above unit T3 lie sandstone-dominated strata deposited during regressions, respectively called units R2 and R3 by Wright (1986), Wright-Dunbar (1992), and Wright and Hayden (1988). Below the T2 marker shale lie interbedded sandstones and mudstones (R1 unit) that constitute an 8-m-thick transition zone above the Mancos Shale (Figs. 9 and 10).

Below, I describe the sedimentologic characteristics of these units in ascending order, beginning with the upper Mancos Shale (Satan Tongue). The Bosque Grande stratigraphic section covers the lower half of the Point Lookout Sandstone, extending 36 m to a stratigraphic position 6 m above the "marker shale" (Figs. 9 and 11, near top of R2). The previously published Point Balcon section extends 22 m above the "marker shale" (Fig. 12; Wright and Hayden, 1988; Wright-Dunbar, 1992).

The upper Mancos Shale (lower ~7 m of Fig. 11, units BG-01 through BG-02) consists of dark-gray to dark-grayish-brown claystone, silty claystone, and subordinate beds of lower-very-fine to upper-fine sandstone and clayey-silty very fine sandstone. Strata are laminated to very thinly bedded and horizontal-planar to slightly wavy; bedding is well defined, typically with sharp bases and tops. A ~20-cm-thick sandstone bed seen 50 m west of the Bosque Grande stratigraphic section exhibits hummocky cross-stratification (Second-Day Road Log, fig. 2.26). Locally, lamina are disrupted or exhibit minor soft-sediment deformation. Sandstone beds lack sedimentary structures, and burrows were not noted. Both clayey sediment and sands are interpreted to have been deposited by settling from hypopycnal flows or from offshore-directed, storm-generated currents (including hyperpycnal flows). The general paucity of hummocky cross-stratification, no burrow trace fossils, and the predominance of mudstone compared to very fine sandstone indicate an offshore to offshore-transition depositional environment.

The Mancos-Point Lookout transition zone is characterized by interbedded mudstones, siltstones, and sandstones (Fig. 11, BG-03 through BG-13). Most strata are in laminated to very thin, tabular beds. About 10% of beds are 3–15-cm-thick siltstones to very fine sandstones that have lenticular or channel-like geometric forms; these are massive to laminated (horizontal-planar to hummocky cross-stratified). The lower ~8 m represents the upper part of a coarsening-upward parasequence (P-1a; Fig. 11, units BG-03 to BG-08), corresponding to a subdivision of the Wright-Dunbar R1 unit that I call R1a. A mudstone-dominated interval is found at 15.3–17.6 m (Fig. 11, units BG-09 and T1b), which grades upward into an interval comprising sandstones and siltstones interbedded with subordinate mudstones (Fig. 11, BG-10 to BG-13); this upward coarsening corresponds to Parasequence 1b (R1b in the

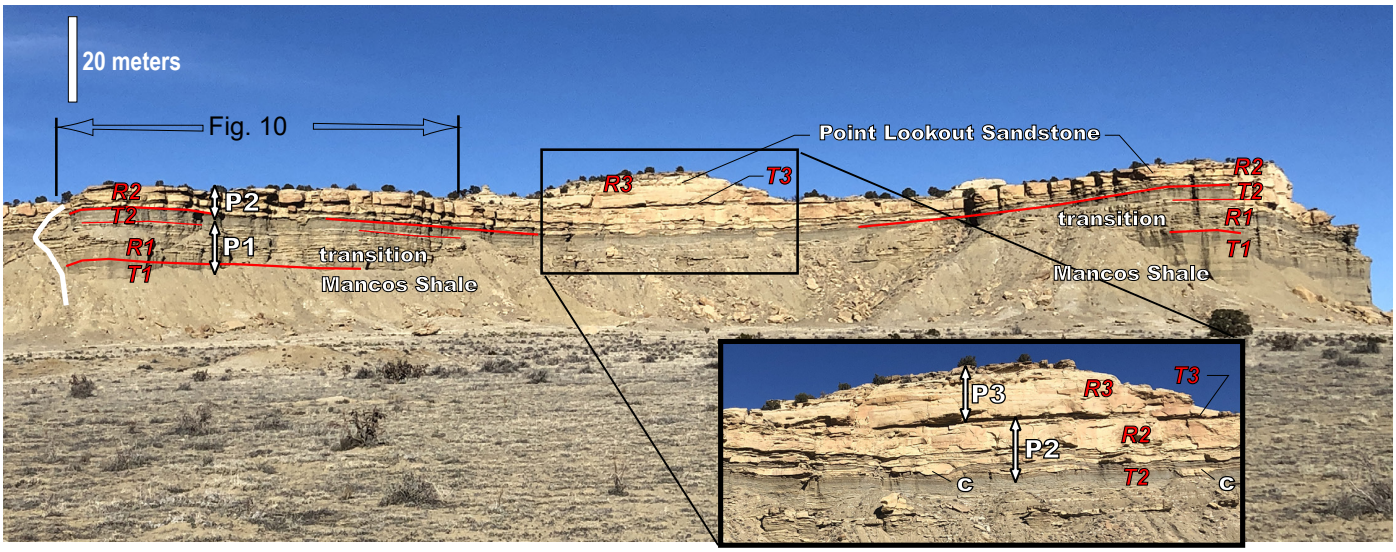


FIGURE 9. Outcrop showing the Point Lookout Sandstone and its transition into the underlying Mancos Shale (Satan Tongue). The white line is the location of the Bosque Grande stratigraphic section (Fig. 11). Red lines and text note the transgressive-regressive lithologic units of Wright (1986) that correspond to mudstone-rich strata deposited during transgressions (T1, T2) and sandstone-rich strata deposited during regressions (R1, R2). T2 corresponds to the "marker shale" of Wright (1986) and Wright and Hayden (1988). Location corresponds to Stop 1A of the Second-Day Road Log of this field conference. Parasequences are annotated by white double-sided arrows and labeled P-1 and P-2.

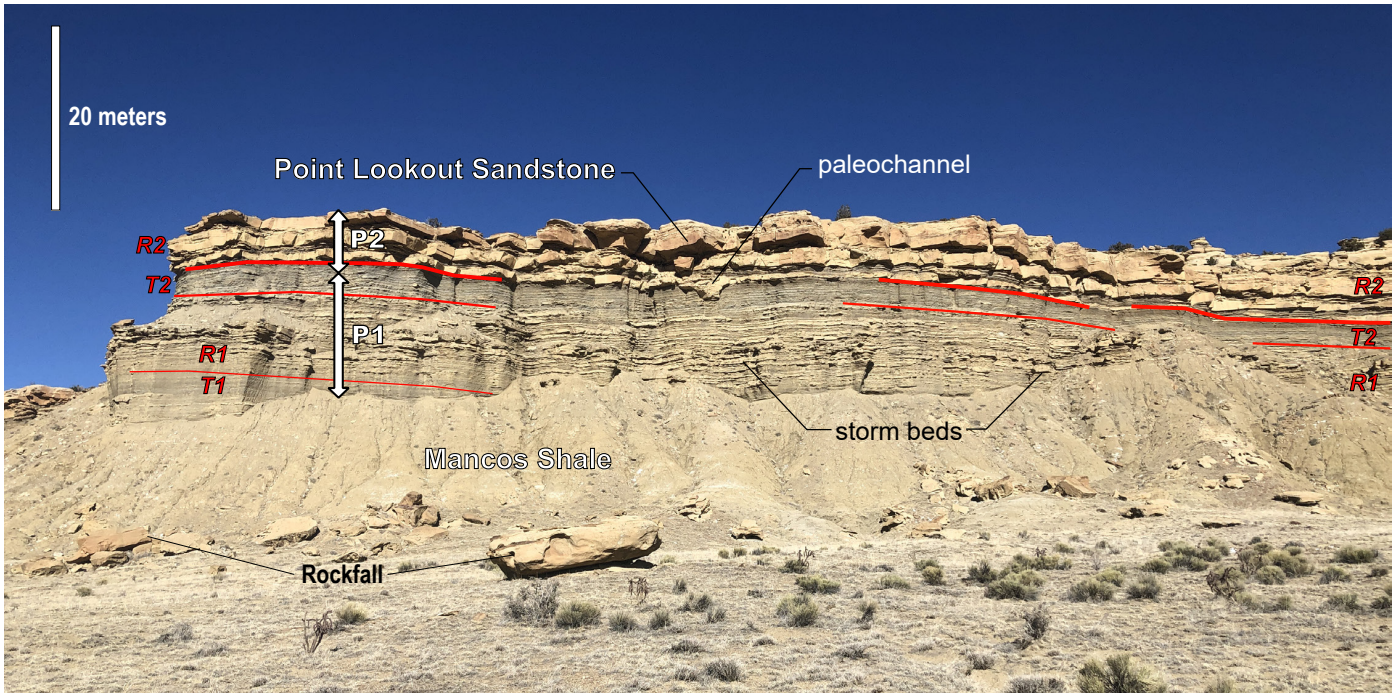


FIGURE 10. Close-up photo of the western side of the outcrop face shown in Figure 9. Parasequences are annotated by white double-sided arrows and labeled P-1 and P-2. Note the lenticular storm beds in the R1 lithologic unit and the paleochannel cutting into the T2 unit. Relatively deep paleochannels (gutter casts) are found in R1 and R2.

transgressive-regressive nomenclature of Wright-Dunbar). The strata in Parasequence 1b are in laminated to very thin beds, typically tabular beds; however, there are also notable thicker sandstone beds, up to 70 cm thick, that are lenticular or channel-shaped (Fig. 13, bottom panel). These thicker sandstones (lower-very-fine to lower-fine grain size) either lack sedimentary structures (massive) or exhibit laminations that are horizontal-planar or suggestive of gentle swaly to hummocky cross-laminations (HCS). Commonly, the uppermost part of the beds have the best-defined laminations and HCS. The lenticular and channel-shaped sandstones, having scoured basal contacts and sharp tops often capped by HCS, are interpreted as storm deposits according to criteria in Lin and Bhattacharya (2021). Bioturbation, particularly burrows, are very minor compared to that seen above the T2 "marker shale." Relatively abundant organic debris, most commonly seen on bedding or lamination surfaces, is up to 2–3 mm long and suggests a nearby fluvial delta (Wright and Hayden, 1988). Proximity to deltaic distributary channels can also explain the relatively high number of storm beds and paleochannels (Lin and Bhattacharya, 2021). The relatively high amount of organic debris, local ball-and-pillow(?) structures, and the interbedded mudstone-sandstone stratigraphic character is also consistent with deltaic-influenced deposition (i.e., similar to the prodelta facies of Lin and Bhattacharya, 2020).

The marker shale (Fig. 11, units BG-14 and BG-15, transgressive unit T2) is composed of three subunits. The lower 2.5 m (BG-14) consists of very thinly bedded clay, silty clay, and 30% very fine sandstone-siltstone, the proportion of the latter decreasing slightly upsection. The middle 0.6 m consists of 0.5- to 1-cm-thick (locally 2 cm) beds of grayish, silty mudstone; beds are locally finely laminated but also bioturbated (Wright and Hayden, 1988), although distinct burrows were not seen. The upper 0.3 m is browner and displays an upsection increase in the proportion (10–25%) of interbedded very fine sandstones and siltstones relative to mudstones (Fig. 11). Overall, ichnofossils are less abundant in the T2 marker shale compared to the overlying R2 unit. As noted by Wright-Dunbar (1992), the lower 2.5 m probably records deposition during a transgression, with the middle subunit recording maximum water depths. I interpret that the upper part of the T2 unit reflects a shallowing-upward trend at the base of the next parasequence, P-2 (Fig. 11).

Above the marker shale is the ~22-m-thick main body of the Point Lookout Sandstone, which contains two parasequences, P-2 and S-3 (Figs. 11 and 12). The sandstone in the lower-middle part of the main body (Fig. 11, units BG-16 to BG-19; Fig. 12, units PB-3a to PB-4) is massive or locally hummocky cross-stratified, horizontal-planar laminated, or low-angle cross-laminated; *Skilothos* and *Thalassinoides* burrows are present locally. The main body is inferred to have been deposited in the distal to proximal lower shoreface (Figs. 11 and 12).

The abrupt contact between the marker mudstone and the base of the main Point Lookout body represents shoreface downlap of the sandstone-dominated, regressive R2 unit onto the mudstone-dominated, transgressive unit T2 (Wright-Dunbar, 1992). Bedding is thicker in the R2 unit compared to the R1 unit, and these beds typically have scoured lower contacts with relatively abundant toolmarks and gutter casts (Fig. 11). Paleochannel fills are common at the base and in the lower 4 m of the R2 unit (Figs. 11 and 13). These paleochannels are up to 0.9 m deep and filled by lower-fine to upper-fine sandstones. Bidirec-

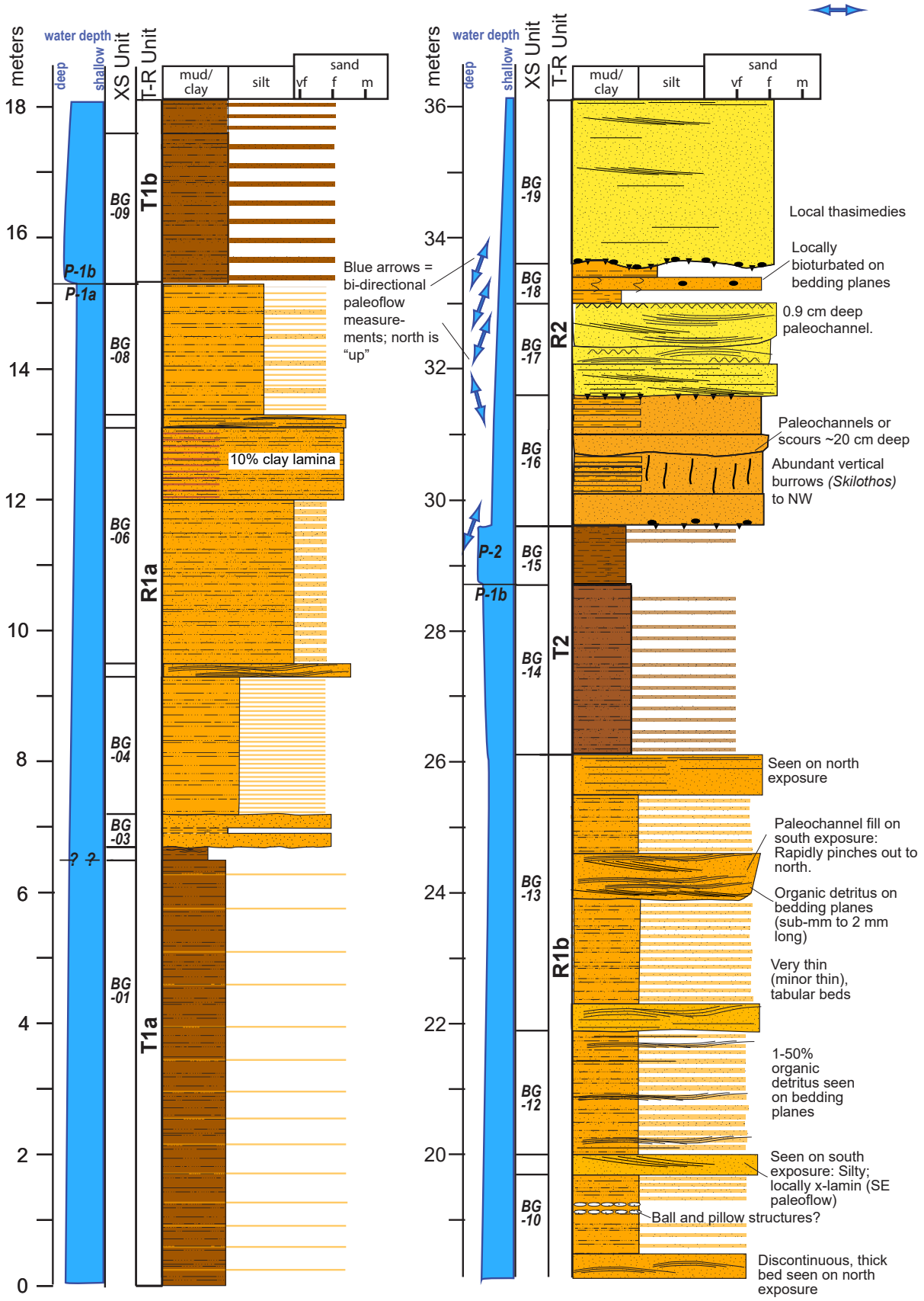


FIGURE 11. Bosque Grande stratigraphic section, encompassing the lower part of the main Point Lookout body and the Point Lookout-Mancos Shale transition. The key for symbols and colors is given in Figure 12. Note the two categories of lithologic units: detailed units specific to this stratigraphic-section (BG-1 through BG-19) and more generalized lithologic units corresponding to transgressions and regressions discussed in previous publications of Wright-Dunbar ("T-R" units labeled T1, R1, T2, R2). Interpreted parasequences are labeled P-1a, P-1b, and P-2.

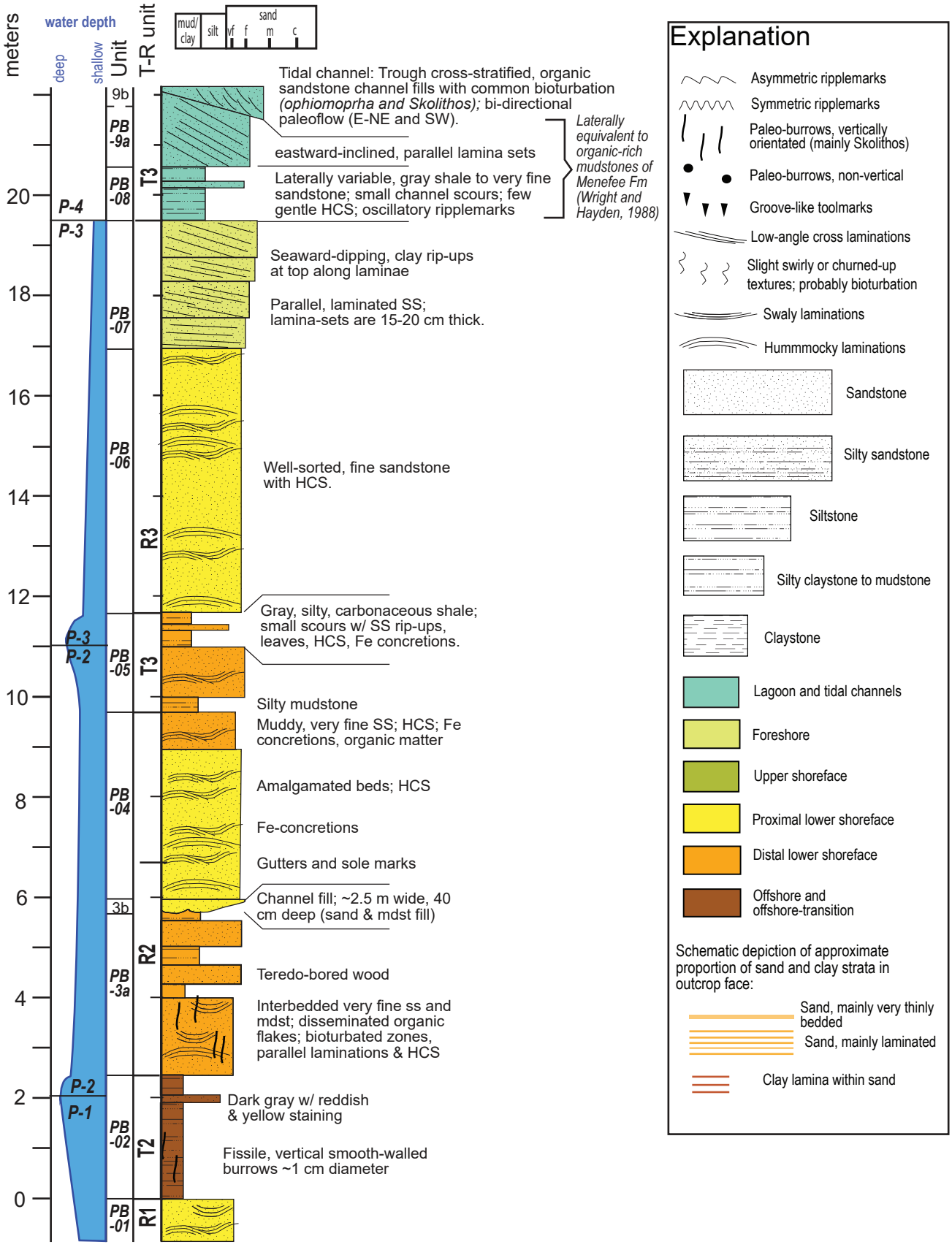


FIGURE 12. The Point Balcon stratigraphic section of Wright and Hayden (1988), modified slightly from Wright-Dunbar (1992, fig. 1.13). Note the two categories of lithologic units: detailed units specific to this stratigraphic-section (PB-01 through PB-09) and more generalized lithologic units corresponding to transgressions and regressions discussed in previous publications of Wright-Dunbar ("T-R" units labeled R1, T2, R2, T3, R3, T4). The explanation applies to all stratigraphic sections (Figs. 8, 11, and 12). Interpreted parasequences are labeled P-1 through P-4.

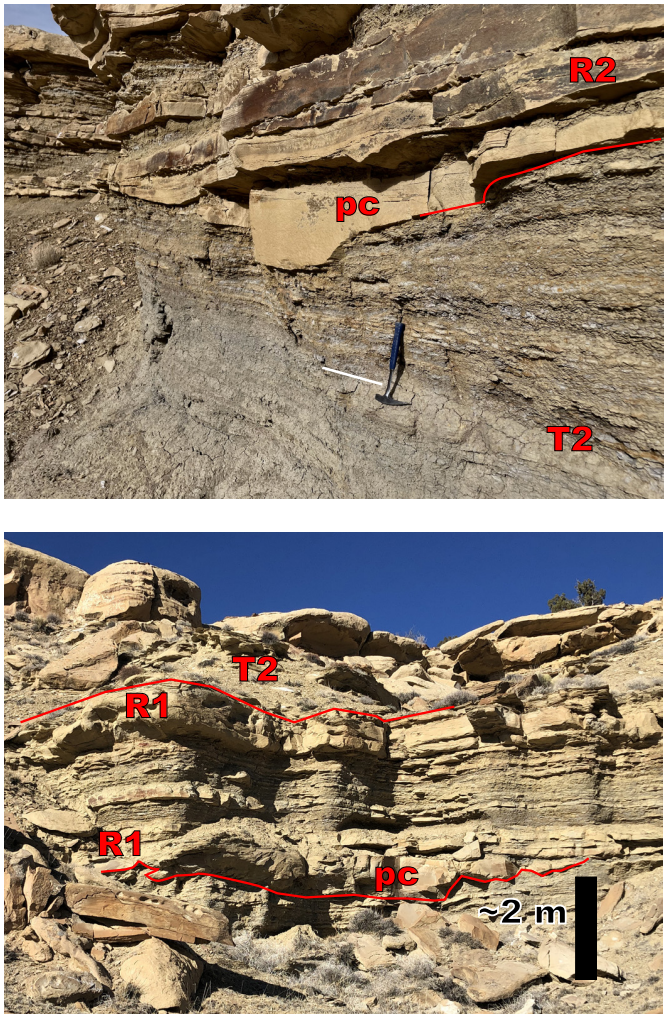


FIGURE 13. Top panel: Close-up of the upper T2 transgressive unit of Wright (1986), scoured into by an overlying paleochannel (pc), the latter called gutter casts by Lin and Bhattacharya (2021), with rock hammer for scale. The contact between T2 and R2 is abrupt and possibly represents a forced regression. In T2, the finest-grained strata are below the white line; above there are higher proportions (~20%) of siltstones and very fine sandstones. The base of the P-2 parasequence is at this white line. Lower panel: Photograph of the R1 unit, with a notable paleochannel (gutter cast) about 3 m below the T2 marker shale.

tional paleoflow measurements of paleochannels, gutter casts, and groove casts range from 340° to 020° (with north-northeast trends being more common in the Bosque Grande stratigraphic section), agreeing with paleoflow data in Wright and Hayden (1988). The relatively thick parasequences, abundance of paleochannels, gutter casts, and toolmarks, as well as the abrupt increase in sandstones at the R2/T2 contact imply a strong influence of a nearby storm-flood-dominated delta deposited during a highstand (Lin and Bhattacharya, 2021). A forced regression at the base of R2 is possible but requires confirmation of a laterally extensive, sharp-based shoreface deposit. The relative abundance of ichnofossils, especially burrows, in R2 compared to T2 and R1 (Fig. 11) implies shallower and more oxygenated water in R2, consistent with a shallower water depth compared to R1.

Descriptions of strata above R2 are from Wright and Hayden (1988) and Wright-Dunbar (1992). A 0.5-m-thick mudstone-rich unit splits the main sandstone body into two parts and consists of gray, silty, carbonaceous shale with sandstone rip-ups, leaf imprints, and HCS (Fig. 12, unit PB-5). This mudstone-rich unit appears to fine-upward and is interpreted to represent deposition during a transgression. The boundary between Parasequences 2 and 3 is placed at the middle of the mudstone-rich unit, above a ~1-m-thick sandstone with HCS (Fig. 12). At the top of Parasequence 3 (Fig. 12, unit PB-7), there is fine- to medium-grained sandstone exhibiting inclined, planar laminated sets, interpreted as a foreshore environment (Fig. 12; Wright-Dunbar, 1992; Dunbar and Hayden, 1988).

The uppermost 4–5 m of the Point Balcon stratigraphic section consists of muddy sandstones and mudstones (Fig. 12, unit PB-8) capped by trough cross-stratified sandstone channel fills (Fig 12, unit PB- 9). Unit PB-8 is 1 m thick and highly variable in a lateral sense, ranging from gray shale to sandstone beds with oscillation ripples to channeled, carbonaceous sandstones; locally there is HCS. The foresets in the uppermost channel fill (unit PB-9) are bidirectional, and *Ophiomorpha* and *Skolithos* trace fossils are relatively common; this channel fill is interpreted as belonging to a tidal channel (Wright and Hayden, 1988). Units 8 and 9 are in the same stratigraphic position as organic mudstones of the Menefee Formation to the west-southwest and were interpreted as a lagoon or tidal flat environment (Wright and Hayden, 1988). Unit PB-8 can alternatively be interpreted as a low-energy, longshore trough on the upper shoreface or lower shoreface, in which case unit PB-9a may represent the longshore bar (Wright and Hayden, 1988).

## DISCUSSION

The Point Lookout and Gallup sandstones both were deposited during long-term regression of the southwestern shoreline of the WIS, as indicated by the overall shallowing of nearshore facies and the progressive upsection increase in the proportion of sandstone to mudstone. Based on hand lens inspection, the sandstones are relatively similar in composition and texture.

There are marked differences between the two units. One difference is that in the Point Lookout Sandstone, vertical aggradation characterized the early deposition (resulting in ~15-m-thick Parasequences 1a and 1b), followed by notable progradation (upward-shallowing) events associated with Parasequences 2 and 3. Above the marker shale in the Point Lookout Sandstone, there appear to be major swings of apparent water depths and depositional environments, as evidenced by the mudstone-sandstone couplets (T2-R2, T3-R3), but this interpretation is complicated by what is likely to be episodic high fluxes of sediment during deltaic flood events (Lin and Bhattacharya, 2021). The 8–9 m thickness of Parasequences 2 and 3, approximately coinciding with the T2-R2 and T3-R3 couplets, are notably thinner than lower in the section. Therefore, deposition and accommodation of the Point Lookout is characterized by aggradation followed by progradation, consistent with previous interpretations of it being associated with a highstand systems tract (Wright and Hayden, 1988).

Interbedded mudstones are lacking in the Gallup Sandstone at Guadalupe Ruin. The most dramatic shift in water depth at the Guadalupe Ruin section occurred in Parasequence 2 (Fig. 8, units 3c–6), which is 10 m thick (note that this is not the same Parasequence 2 as discussed in the Point Lookout Sandstone). Deciphering parasequences in the overlying 13 m of the unit is uncertain, and water depth there seems to be relatively constant based on the similarity of lithofacies (Fig. 8). So deposition and accommodation of the Gallup Sandstone are characterized by progradation (Parasequence 2) followed by aggradation (Parasequence 3).

Correlating the Guadalupe Ruin site with the distalmost Gallup Sandstone studied by Lin et al. (2019) suggests an approximate match of the thicknesses of the lower three parasequences (Fig. 14). Such a comparison is problematic, however, due to the 200 km of distance between the two sites, so only tentative inferences can be made. Parasequence 4 seems to be above their Gallup Sandstone, and I did not observe the Tocito Sandstone in my stratigraphic section, possibly because the Gallup Sandstone is thicker at Guadalupe Ruin and its stratigraphic section did not extend far enough upward to capture the Tocito (cf. Nummedal and Molenaar, 1995, fig. 6). The most important inference made by this comparison is that Lin et al. (2019) interpreted the interval that appears to correlate to the lower two parasequences at Guadalupe Ruin to be deposited during the progradation of a highstand systems tract (Lin's parasequences 4a through 4e) and the overlying strata to be associated with aggradation during an inferred lowstand systems tract (Lin's parasequences 3a and 3b).

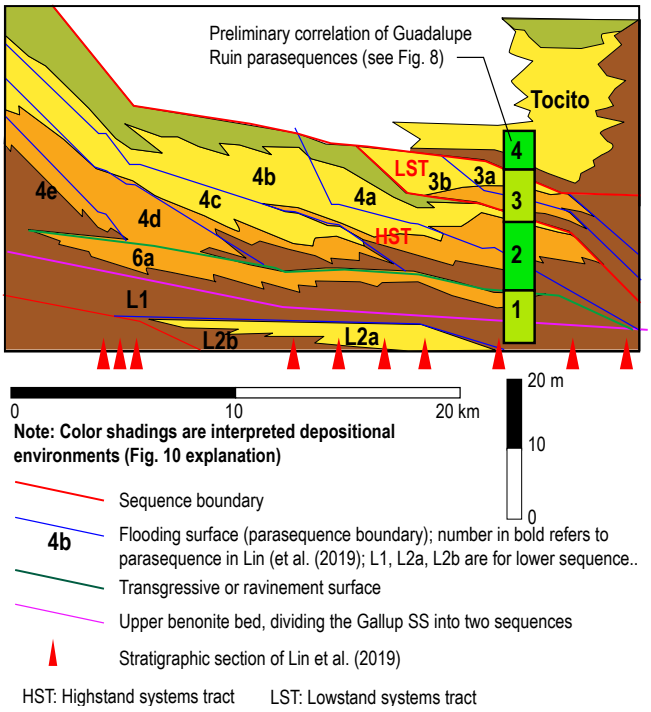


FIGURE 14. Most distal Gallup Sandstone tongue stratigraphy, interpreted by Lin et al. (2019) for outcrops 200 km northwest of the study area. The scaled green column shows a possible correlation of the parasequences inferred for the Guadalupe Ruin stratigraphic section. Such a long distance makes correlations tentative, but it is intriguing that boundaries between the lower three parasequences in the Guadalupe stratigraphic section approximately match Lin's parasequences and their bounding flooding surfaces. This comparison suggests that Parasequences 1 and 2 in Guadalupe Ruin are associated with a highstand systems tract, whereas the overlying sandstones are associated with an inferred lowstand systems tract, which is supported by the progradation-aggradation accommodation trend seen at Guadalupe Ruin. Note that the Tocito Sandstone was not observed in the Guadalupe Ruin stratigraphic section.

Another contrast between the Point Lookout and Gallup Sandstone tongues is the abundance of storm-related, lenticular to channel-shaped beds in the lower part of the Point Lookout Sandstone, especially in the ~4 m above and below the T2 marker shale. It is interpreted that strong storm-related currents, probably in conjunction with high sediment and water discharges from a nearby delta distributary channel, generated these types of beds (Wright and Hayden, 1988; Wright-Dunbar, 1992) and were also likely responsible for gutter casts and grooves seen at the bases of both channelized and tabular sandstone beds.

This study only focused on two specific areas. Much more detailed stratigraphic study is needed to answer these questions, but I hypothesize these differences may relate to two factors: (1) coastline morphologies changing with varying sea-level stages, as conceptually modeled by sequence stratigraphy, and (2) proximity to a deltaic distributary channel for the two time periods associated with the Point Lookout and upper Gallup Sandstones. Detailed study of the Point Lookout Sandstone has indicated it was deposited during a general highstand systems tract (Wright and Hayden, 1988). This inference is corroborated by progressively rising global sea levels during 84–81 Ma, with short-term sea-level drops being less than in the Coniacian (Fig. 4; Haq, 2014). High-frequency transgressions during this time resulted in the formation of lagoons, tidal flats, and associated tidal channels in addition to the drowning of river valleys and the drowning forming estuaries (Wright, 1986; Devine, 1991; Katzman and Wright-Dunbar, 1992). These and relatively stable barrier island-lagoon complexes that characterize a transgression resulted in trapping of fluvially inputted sand (Wright, 1986; Devine, 1991), facilitating mudstone deposition on the former shoreface and resulting in the laterally continuous mudstone tongues T1, T2, and T3 (Wright, 1986). Large estuaries and/or lagoons perhaps allows relatively higher short-term surging/discharging outflow from back-barrier features following storm events, facilitating paleochannel (gutter cast) development along with toolmarks before and after maximum sea level (apparently the water depth was too deep during the peak of the transgression to have these strong-current features). Development of paleochannels (with HCS in their upper fills), gutter casts, and toolmarks may also be promoted due to proximity to deltaic distributary channels that experienced storm-related surges in discharge (Lin and Bhattacharya, 2021). Such proximity is inferred from the presence of deltaic (i.e., prodelta) features in the lower part and transitional base of the Point Lookout in the Bosque Grande section (R1 and R2), such as organic detritus, possible ball-and-pillow features, and interbedded sandstones and mudstone (cf. Lin and Bhattacharya, 2020).

Aspects of coastline morphology, influenced by sea-level changes, and happenstance distance to major deltaic distributary channels may explain the stratigraphic character of the

Gallup Sandstone observed at Guadalupe Ruin. If Parasequences 3a and 3b of the Gallup Sandstone were deposited in a lowstand systems tract, as inferred for the upper, basinward end of the Gallup 200 km to the northwest (Fig. 14; Lin et al., 2019), and consistent with a progradation-aggradation stacking pattern observed here, one would expect incised valleys and minimal development of lagoons and tidal flats. Such a scenario would facilitate sediment bypass of the coastal margin and promote the aggradation of the middle-upper Gallup Sandstone (Parasequences 3a and 3b). Aggradation rates might have been sufficiently high that the middle-upper Gallup Sandstone is actually a single parasequence and a high-frequency transgression is not recorded in this stratigraphic interval at Guadalupe Ruin. Or perhaps a quasi-static coastline associated with a lowstand system tract, "pinned" by clinoforms associated with the underlying sequence, retarded lateral shifts of depositional facies, inhibiting aggradation of thick mudstone tongues in the middle-upper Gallup Sandstone. The lack of deep paleochannels, lenticular beds, and strong-current features in the Gallup might relate to: (1) long distances from deltaic distributary channels or (2) lack of back-barrier stormwater storage (in estuaries or lagoons) and corresponding lack of post-storm outflow. The first factor is likely due to happenstance, but the second would be a result of a sea-level lowstand. One cannot negate the possibility of differences in paleoclimate, with lower frequency or intensity of storms in the early Coniacian versus the early Campanian, but much more data would be needed to support such a hypothesis.

## CONCLUSION

This study compares the Gallup and Point Lookout Sandstones in the Cabezon area, located 70 km northwest of Albuquerque in the middle Rio Puerco Valley. Both represent regression of the WIS shoreline during two different times in the Late Cretaceous (early Coniacian versus early Campanian), and the thickness of the main sandstone bodies are approximately similar (18–22 m). However, the Gallup and Point Lookout Sandstones have two intriguing differences. First, storm-related channel-fill sandstones and lenticular beds, having highly scoured bases with gutter casts and toolmarks (oriented 340° to 020°, with north-northeast trends being more common), are much more abundant in the Point Lookout Sandstone than the Gallup Sandstone, especially in the lower part of the Point Lookout (R1 and R2 units). Second, parasequences are more obvious in the Point Lookout Sandstone, where laterally continuous mudstones (several km long and up to 3 m thick) transition upward into sandstones, resulting in mudstone-sandstone couplets that record high-frequency (5th-order) deepening (transgression) events followed by shallowing (regressions). Except for its lower part, the Gallup Sandstone at Guadalupe Ruin lacks obvious parasequences and related mudstone-sandstone couplets. Much of these differences can be explained by differences in shoreline morphology due to contrasting sea-level states of the Point Lookout and Gallup Sandstones, as conceptually modeled by sequence stratigraphy. The Point Lookout Sandstone was mainly deposited during a sea-level highstand (Wright, 1986; Wright and Hayden, 1988), consistent with its aggradation-progradation accommodation (stacking) character. Deposition of transgressive mudstone lower in a parasequence was facilitated by the trapping of sand in estuaries and lagoons, the widespread occurrence of which would be expected in a highstand and the presence of which has been previously interpreted in the local stratigraphic record (e.g., Devin, 1991; Katzman and Wright-Dunbar, 1992). Storm-related discharges of water and sediment from nearby deltaic distributary channels promoted paleochannels, gutter casts, and toolmarks. The studied Gallup Sandstone (A tongue of Nummedal and Molenaar, 1995) appears to have a progradation-aggradation accommodation character, consistent with deposition in a highstand (lower part of unit) followed by a deposition in a lowstand (middle-upper part of unit), as previously inferred by Lin et al. (2019) for the most basinward extent of the upper Gallup Sandstone 200 km to the northwest. A postulated lowstand inferred for the middle-upper Gallup (for this studied part of the A tongue) would theoretically lack estuary and lagoon back-barrier features (Lin and Bhattacharya, 2020) and promote channeled fluvial systems on the coastal margin; this could increase shoreline sand aggradation rates and reduce sand storage during 5th-order transgressions, both of which might inhibit mudstone deposition and obscure recognitions of parasequences in the middle-upper Gallup Sandstone. The shoreface lithofacies associations and lack of deltaic features in the Gallup at the Guadalupe section indicate a happenstance far distance from deltaic channels. This distance and lack of back-barrier storage would reduce the likelihood of forming storm-related features such as paleochannels, gutter casts, and toolmarks.

## ACKNOWLEDGMENTS

I would like to thank the two reviewers of this paper, Wen Lin and Lawrence Tanner. Maya Elrick provided thoughtful discussions in the field and also edited related material in the Second-Day Road Log. Claire Koning assisted in measuring the Bosque Grande stratigraphic section.

## REFERENCES

Bourdon, J., Wright, K., Lucas, S.G., Spielmann, J., and Pence, R., 2011, Selachians from the Upper Cretaceous (Santonian) Hosta Tongue of the Point Lookout Sandstone, central New Mexico: New Mexico Museum of Natural History and Science Bulletin 52, 54 p.

Campbell, C.V., 1971, Depositional model: upper Cretaceous Gallup beach shoreline, Shiprock area, northwestern New Mexico: Journal of Sedimentary Petrology, v. 41, p. 395–409.

Campbell, C.V., 1973, Offshore equivalents of Upper Cretaceous Gallup beach sandstones, northwestern New Mexico, *in* Fassett, J.E., ed., Cretaceous and Tertiary Rocks of the Southern Colorado Plateau: Four Corners Geological Society, p. 78–84.

Campbell, C.V., 1979, Model for beach shoreline in Gallup Sandstone (Upper Cretaceous) of northwestern New Mexico: New Mexico Bureau of Mines and Mineral Resources Circular 164, 32 p.

Devine, P.E., 1991, Transgressive origin of channeled estuarine deposits in the Point Lookout Sandstone, northwestern New Mexico: A model for Upper Cretaceous, cyclic regressive parasequences of the U.S. Western Interior: American Association of Petroleum Geologists Bulletin, v. 75, no. 6, p. 1039–1063.

Gardner, M.H., 1995, Tectonic and eustatic controls on the stratal architecture of Mid- Cretaceous stratigraphic sequences, central Western Interior Foreland Basin of North America, *in* Dorobek, S.L., and Ross, G.M., eds., Stratigraphic Evolution of Foreland Basins: SEPM Special Publication 52, p. 243–281.

Haq, B.U., 2014, Cretaceous eustasy revisited: Global and Planetary Change, v. 113, p. 44– 58.

Hunt, C.B., 1936, Geology and fuel resources of the southern part of the San Juan Basin, New Mexico, Part 2: The Mount Taylor coal field: U.S. Geological Survey Bulletin 860-B, 80 p.

Johnson, S.C., and Lucas, S.G., 2003, Selachian fauna from the Upper Cretaceous Dalton Sandstone, middle Rio Puerco Valley, New Mexico, *in* Lucas, S.G., Semken, S.C., Berglof, W., and Ulmer-Scholle, D., eds., Geology of the Zuni Plateau: New Mexico Geological Society Guidebook 54, p. 353–358.

Katzman, D., and Wright-Dunbar, R., 1992, Parasequence geometry and facies architecture in the Upper Cretaceous Point Lookout Sandstone, Four Corners platform, southwestern Colorado, *in* Lucas, S.G., Kues, B.S., Williamson, T.E., and Hunt, A.P., eds., San Juan Basin IV: New Mexico Geological Society Guidebook 43, p. 187–197.

Koning, D.J., 2024, Second-day road log: From Bernalillo to San Ysidro, around southern Nacimiento Mountains, to San Luis and Guadalupe in the Middle Rio Puerco Valley, *in* Karlstrom, K.E., Koning, D.J., Lucas, S.G., Iverson, N.A., Crumpler, L.S., Aubele, J.C., Blake, J.M., Goff, F., and Kelley, S.A., eds., Geology of the Nacimiento Mountains and Río Puerco Valley: New Mexico Geological Society Guidebook 74 (this volume), p. 201–217.

Koning, D.J., and Jochems, A.P., 2014, Geologic map of the Benavidez Ranch 7.5-minute quadrangle, Bernalillo and Sandoval Counties, New Mexico: New Mexico Bureau of Geology and Mineral Resources Open-File Geologic Map 234, scale 1:24,000.

Koning, D.J., and Rawling, G., 2017, Geologic map of the San Felipe Mesa 7.5-minute quadrangle, Sandoval County, New Mexico: New Mexico Bureau of Geology and Mineral Resources Open-File Geologic Map 266, scale 1:24,000.

Lin, W., and Bhattacharya, J.P., 2020, Depositional facies and the sequence stratigraphic control of a mixed-process influenced clastic wedge of the Cretaceous Western Interior Seaway: The Gallup System, New Mexico, USA: Sedimentology, v. 67, p. 920–950, https://doi.org/10.1111/sed.12667

Lin, W., and Bhattacharya, J.P., 2021, Storm-flood-dominated delta: A new type of delta in stormy oceans: Sedimentology, v. 68, p. 1109–1136.

Lin, W., Bhattacharya, J.P., and Stockford, A., 2019, High-resolution sequence stratigraphy and implications for Cretaceous glacioeustacy of the Late Cretaceous Gallup System, New Mexico, U.S.A.: Journal of Sedimentary Research, v. 89, no. 6, p. 552–575, https://doi.org/10.2110/jsr.2019.32

Molenaar, C.M., 1973, Sedimentary facies and correlation of the Gallup Sandstone and associated formations, northwestern New Mexico, *in* Fassett, J.E., ed., Cretaceous and Tertiary Rocks of the Southern Colorado Plateau: Four Corners Geological Society, p. 85–110.

Molenaar C.M., 1983, Principal reference section and correlation of the Gallup Sandstone, northwestern New Mexico, *in* Hook, S.C., compiler, Contributions to mid-Cretaceous paleontology and stratigraphy of New Mexico: New Mexico Bureau of Mines and Mineral Resources Circular 185, p. 29–40.

New Mexico Bureau of Geology and Mineral Resources, 2003, Geologic map of New Mexico, scale 1:500,000, 2 sheets, https://doi.org/10.58799/116894

Nummedal, D., 1990, Sequence stratigraphic analysis of upper Turonian and Coniacian strata in the San Juan Basin, New Mexico, USA, *in* Ginsburg, R.N., and Beaudoin, B., eds., Cretaceous Resources, Events and Rhythms: Backgrounds and Plans for Research: Dordrecht, Kluwer Publishing, p. 33–46.

Nummedal, D., 2004, Tectonic and eustatic controls on Upper Cretaceous stratigraphy of northern New Mexico, *in* Mack, G.H., and Giles, K.A., The Geology of New Mexico, A Geologic History: New Mexico Geological Society Special Publication 11, p. 169–182.

Nummedal, D., and Molenaar, C.M., 1995, Sequence stratigraphy of ramp-setting strand plain successions: The Gallup Sandstone, New Mexico, *in* van Wagoner, J.C., and Bertram, G.T., eds., Sequences Stratigraphy of Foreland Basin Deposits: American Association of Petroleum Geologists Memoir 64, p. 277–310, https://doi.org/10.1306/M64594C10

Nummedal, D., and Riley, G.W., 1991, Origin of late Turonian and Coniacian unconformities in the San Juan Basin, *in* J.C. van Wagoner, J.C., Nummedal, D., Jones, C.R., Taylor, D.R., Jennette, D.C., and Riley, G.W., eds., Sequence stratigraphy applications to shelf sandstone reservoirs—outcrop to subsurface examples: AAPG Field Conference, September 21–28, 1991 (not consecutively paginated), p. 1–12.

Nummedal, D., and Swift, D.J.P., 1987, Transgressive stratigraphy at sequence-bounding unconformities: Some principles derived from Holocene and Cretaceous samples, *in* Nummedal, D., Pilkey, O.H., and Howard, J.D., eds., Sea-level Fluctuation and Coastal Evolution: SEPM Special Publication 41, p. 241–260.

Pemberton, S.G., MacEachern, J.A., Dashtgard, S.E., Bann, K.L., Gingras, M.K., and Zonneveld, J.-P., 2012, Chapter 19: Shorefaces, *in* van Loon, A.J., ed., Developments in Sedimentology, vol. 64, p. 563–603, https://doi.org/10.1016/B978-0-444-53813-0.00019-8

Posamentier, H.W., Jervey, M.T., and Vail, P.R., 1988, Eustatic controls on clastic deposition I: Conceptual framework, *in* Wilgus, C.K., Hastings, B.S., Ross, C.A., Posamentier, H., van Wagoner, J., and Kendall, C.G. St. C., eds., Sea-Level Changes: An Integrated Approach: SEPM Special Publication 42, p. 109–124.

Rawling, G.C., and Koning, D.J., 2019, Geologic map of the Herrera 7.5-minute quadrangle, Sandoval and Bernalillo Counties, New Mexico: New Mexico Bureau of Geology and Mineral Resources Open-File Geologic Map 273, scale 1:24,000.

Sealey, P.L., and Lucas, S.G., 2019, Late Cretaceous (Cenomanian-Campanian) ammonite systematic paleontology and biostratigraphy, southeastern San Juan Basin, Sandoval County, New Mexico: New Mexico Museum of Natural History and Science Bulletin 80, 245 p.

Sears, J.D., 1925, Geology and coal resources of the Gallup-Zuni basin, New Mexico: U.S. Geological Survey Bulletin 767: Washington, D.C., Government Printing Office, no. 767, 138 p.

SepmStrata, 2024, Clastic system tracts in perspective, evolution of coastal regions as sea level changes and controls the accommodation [video]: https://www.youtube.com/watch?v=d8-tsz9P5Oo, accessed February 16, 2024.

Shetiwy, M.M., 1978, Sedimentologic and stratigraphic analysis of the Point Lookout Sandstone, southeast San Juan basin, New Mexico [Ph.D. dissertation]: Socorro, NM, New Mexico Institute of Mining and Technology, 262 p.

Singer, B.S., Jicha, B.R., Sawyer, D.A., Walaszczyk, I., Landman, N., Sageman, B.B., and McKinney, K.C., 2023, A $^{40}Ar/^{39}Ar$ and U-Pb timescale for the Cretaceous Western Interior Basin, North America, *in* Hart, MB., Batenburg, S.J., Huber, B.T., Price, G.D., Thibault, N., Wagreich, M., and Walaszczyk, I., eds., Cretaceous Project 200 Volume 1: The Cretaceous World: Geological Society of London Special Publication 544, https://doi.org/10.1144/SP544-2023-76

Tillman, R.W., 1985, The Tocito and Gallup Sandstones, New Mexico, a comparison, *in* Tillman, R.W., Swift, D.J.P., and Walker, R.G., eds., Shelf Sands and Sandstone Reservoirs: SEPM Short Course 13, p. 403–463.

Van Cappelle, M. Hampson, G.J., and Johnson, H.D., 2018, Spatial and temporal evolution of coastal depositional systems and regional depositional process regimes: Campanian Western Interior Seaway, U.S.A.: Journal of Sedimentary Research, v. 88, p. 873–897.

van Wagoner, J.C., Mitchum, R.M., Jr., Posamentier, H.W., and Vail, P.R., 1987, Seismic stratigraphy interpretation using sequence stratigraphy, part 2: Key definitions of sequence stratigraphy, *in* Bally, A.W., ed., Atlas of Seismic Stratigraphy: AAPG Studies in Geology #27, vol. 1, p. 11–14.

van Wagoner, J.C., Posamentier, H.W., Mitchum, R.M., Jr., Vail, P.R., Sarg, J.F., Loutit, T.S., and Hardenbol., J., 1988, An overview of the fundamentals of sequence stratigraphy and key definitions, *in* Wilgus, C.K., et al., eds., Sea-Level Changes: An Integrated Approach: Tulsa, OK, Society of Economic Paleontologists and Mineralogists Special Publication 42, p. 39–45.

Weimer, R.J., 1984, Presidential Address: Developments in sequence stratigraphy: Foreland and cratonic basins: AAPG Bulletin 76, no. 7, p. 965–982.

Williamson, T.E., and Lucas, S.G., 1992, Selachian fauna from the Upper Cretaceous (Coniacian) El Vado Sandstone Member of the Mancos Shale, San Juan Basin, New Mexico, *in* Lucas, S.G., Kues, B.S., Williamson, T.E., and Hunt, A.P., eds., San Juan Basin IV: New Mexico Geological Society Guidebook 43, p. 17–19, https://doi.org/10.56577/FFC-43

Wright, K., 2013, Seismic stratigraphy and geomorphology of Palaeocene volcanic rocks, Faroe-Shetland Basin [unpublished Ph.D. thesis]: Durham, UK, Durham University.

Wright, R., 1986, Cycle stratigraphy as a paleogeographic too: Point Lookout Sandstone, southeastern San Juan Basin, New Mexico: Geological Society of America Bulletin, v. 96, p. 661–673.

Wright, R., and Hayden, S., 1988, Stop 9: Arroyo Balcon, Point Lookout Sandstone depositional systems, *in* Nummedal, D., Wright, R., and Swift, D.J.P., Sequence Stratigraphy of Upper Cretaceous Strata of the San Juan Basin, New Mexico [field guide]: 73rd AAPG/SEPM Annual Meeting, Houston, TX, p. 116–125

Wright-Dunbar, R., 1992, Shoreline cyclicity and the transgressive record: A model based on Point Lookout Sandstone exposures at San Luis, New Mexico, *in* Lucas, S.G., Kues, B.S., Williamson, T.E., and Hunt, A.P., eds., San Juan Basin IV: New Mexico Geological Society Guidebook 43, p. 12–14.

Wright-Dunbar, R., Zech, R.S., Crandall, G.A., and Katzman, D., 1992, Strandplain and deltaic depositional models for the Point Lookout Sandstone, San Juan Basin and Four Corners platform, New Mexico and Colorado, *in* Lucas, S.G., Kues, B.S., Williamson, T.E., and Hunt, A.P., eds., San Juan Basin IV: New Mexico Geological Society Guidebook 43, p. 199–206.

*Appendices can be found at*
*https://nmgs.nmt.edu/repository/index.cfml?rid=2024005*

Outcrops of Upper Cretaceous Gallup Sandstone along a road south of Cabezon in the southeastern San Juan Basin. *Photo by Spencer G. Lucas*